Histol Histopathol (2022) 37: 1227-1240

http://www.hh.um.es

Histology and Histopathology
From Cell Biology to Tissue Engineering

ORIGINAL ARTICLE **Open Access**

Sphingosine Kinase-1 (SPHK1) promotes inflammation in infantile pneumonia by regulating NLRP3 inflammasome and SIRT1 expression

Niu Ding[1], Yanni Meng[1], Lianhong Liu[1], Song Ma[2] and Yanping Chen[1]

[1]Department of Respiratory Medicine, Hunan Children's Hospital and [2]College of Clinical Medicine, Hunan University of Traditional Chinese Medicine, Changsha, Hunan Province, PR China

Summary. Background. Infantile pneumonia is an acute inflammatory disorder of the lung caused by mycoplasma pneumonia. SPHK1 (sphingosine kinase-1) signaling pathway is involved in the process of inflammatory diseases. However, whether SphK1 regulates inflammatory responses in infantile pneumonia remains unclear. In this study, we investigated the role of SPHK1 in infantile pneumonia and its underlying mechanisms.

Methods. Serum samples of 12 patients with infantile pneumonia and healthy controls were obtained from Hunan Children's Hospital. To induce pneumonia, mice were administrated with LPS (lipopolysaccharide) into the lung. RAW264.7 cells were used as an in vitro macrophage model stimulated with LPS or PBS for 4 h.

Results. SPHK1 mRNA level and protein level in the LPS-treated mice and patients with infantile pneumonia were significantly increased. SPHK1 promoted inflammation and lung injury in mice with infantile pneumonia. The knockdown of SPHK1 expression inhibited inflammation and restrained lung injury in mice with infantile pneumonia. SPHK1 overexpression also exacerbated inflammation in RAW264.7 cells stimulated by LPS, and SPHK1 silencing reduced inflammatory responses. We further showed that SPHK1 induced NLRP3 (NLR Family Pyrin Domain Containing 3) activity by inhibiting SIRT1 expression.

Conclusion. Our study demonstrated that SPHK1 promotes inflammation of infantile pneumonia by modulating NLRP3 inflammasome via the regulation of SIRT1 expression and mitochondrial permeability transition.

Corresponding Author: Yanping Chen, Ph.D., Department of Respiratory Medicine, Hunan Children's Hospital, NO.86 Ziyuan Road, Changsha, Hunan Province, PR China. e-mail: drchenyanping@163.com

DOI: 10.14670/HH-18-491

Key words: SPHK1, Infantile pneumonia, NLRP3, SIRT1

Introduction

Infantile pneumonia is an acute inflammatory disorder in the lung caused by mycoplasma pneumoniae (MP), which is a common pediatric pneumonia accounting for approximately 20% of pneumonia (Xiaomeng et al., 2015). The clinical incidence of MP has been significantly increasing in recent years. Pediatric MP is a contagious disease and is mainly transmitted through the respiratory tract (Li et al., 2019), with a high transmission rate reaching 50% in crowded neighborhood (Zhang et al., 2020). Apart from the respiratory syndromes, the clinical symptoms of infantile pneumonia include encephalitis, nephritis, myocarditis, immune hemolytic anemia and multi-system dysfunction (Tomari et al., 2018; Li et al. 2019).

Recent studies have shown that NLRP3 (NLR Family Pyrin Domain Containing 3) inflammasome plays an extremely important role in the inflammatory responses of acute lung injury (ALI), and NLRP3 is implicated in the initiation and development of acute infectious pneumonia (Liu et al., 2021; Luo et al., 2021b). Elevated NLRP3 activity can cause lung injury by activating NF-κB related pathways, which has been proposed as a potential therapeutic target for lung injury (Pu et al., 2020).

Accumulating evidence has suggested the engagement of SPHK1 signal pathway in the occurrence and development of cancer (Hart et al., 2019). There are also evidence that the activation of SPHK1 signaling pathway in the kidneys of diabetic rats contributes to renal damages including kidney fibrosis and renal inflammation (Lee et al., 2018; Khoei et al., 2020). However, the potential role of SPHK1 signaling in pneumonia remains to be elucidated. In this work, we studied the role of SPHK1 in infantile pneumonia and its

underlying mechanisms.

Materials and methods

Clinical samples

Patients with infantile pneumonia (N=12) and healthy controls (N=12) were obtained from Hunan Children's Hospital from 2018 to 2019. All the participants signed obtained informed consent and the study was approved by the Ethics Committee of Hunan Children's Hospital. Serum of all patients and healthy controls were stored at -80°C freezer until further use.

Animal studies and pneumonia model

A total number of 12 one-week old C57BL/6 mice (male, 4-5 g) were housed separately under controlled temperature (22±3°C), with 50±20% humidity and a light-dark cycle of 12h. Mice were anesthetized by intraperitoneal administration of pentobarbital sodium (50 mg/kg). After anesthetization, mice was injected with 2 mg/kg of LPS (Sigma-Aldrich Merck KGaA) as literature (Li et al., 2019; Pu et al., 2022) into the lung tissues in the pneumonia group. In the sham group, an equal volume of PBS was injected (n=6 in each group). After 3 days, mice were euthanized and the tissue samples were collected. To test the effect of SPHK1, recombinant SPHK1 protein (1 mg/kg) was injected to lung tissues together with LPS administration. To further investigate the role SPHK1 and SIRT1 in mouse model, SPHK1 inhibitor (MP-A08, Sigma) or SIRT1 agonist (CAY10602, Sigma), or SIRT1 inhibitor (Selisistat, Sigma) was injected at 5 mg/kg after LPS administration. To assess the role of ROS in model of infantile pneumonia, ROS inhibitor (5-Galloylquinic acid, Sigma) or ROS agonist (Sideroxylin, Sigma) was applied at 10 mg/kg after LPS administration.

Hematoxylin-Eosin (H&E) Staining

Lung tissue samples were fixed with 4% paraformaldehyde and were paraffin-embedded. Samples were cut into 5 μm sections using a microtome. H&E staining was performed using H&E Stain Kit (ab245880, Abcam). Briefly, deparaffinized and hydrated section was incubated in Hematoxylin staining solution for 5 mins. The section was rinsed twice with distilled water to remove excess stain. Then adequate Bluing Reagent was applied to completely cover tissue section for 30 secs. After washing with distilled water, the section was dehydrated in absolute alcohol and then stained with Eosin Y Solution for 2-3 mins. The images were captured a light microscopy (BH3-MJL; Olympus Corporation, Tokyo, Japan).

Immunofluorescence

Lung tissue samples were fixed with 4% paraformaldehyde and were paraffin-embedded. Samples were cut into 5 μm sections using a microtome and permeabilized with 0.5% Triton X-100. After blocking in 5% goat serum for 1 h, the sections were stained with anti-SPHK1 antibody (1:200, Cell Signaling Technology), overnight at 4°C. After washing, Alexa 594-conjugated secondary antibody (1:200, Thermo Fisher Scientific) was used to label the primary antibody for 1 h at room temperature. After counterstaining with DAPI, the images were taken under a fluorescence microscope (LSM 510 Meta; Carl Zeiss).

Expression plasmids and SPHK1 gene silencing, cell culture and transfection

Human SPHK1 cDNA were amplified by standard PCR from the mRNA sample of RAW264.7 cells. The cDNA sequence was cloned into the pGL3-Basic vector (Promega) for SPHK1 overexpression. Si-RNA targeting SPHK1 (si-SPHK1) and negative control were purchased Santa Cruz Biotechnology. RAW264.7 cells (ATCC) were cultured at 37°C, 5% CO_2 in DMEM containing 10% fetal bovine serum, penicillin (100 U/ml), and streptomycin (100 mg/ml).

RAW264.7 macrophage cells were grown to 80% confluence in 6-well plates and transfected with plasmids (6 μg pGL3-SPHK1 or 200 nM of si-SPHK1 and negative control) by Lipofectamine 2000 (Thermo Fisher Scientific). 48 h post-transfection, RAW264.7 cells were stimulated with 0.1 mg/ml LPS as literature (Li et al., 2019; Pu et al., 2022) or PBS for 4 h before further analysis.

Real-time quantitative RT-PCR

Total cellular RNA was extracted using Trizol reagent (Thermo Fisher Scientific) from lung tissue or cells. The extracted total RNA was dissolved in DEPC water and the concentration was measured with NanoDorp. 1 μg of total RNA was used for reverse-transcription using RevertAid First Strand cDNA Synthesis Kit (Thermo Fisher Scientific). The resulted cDNA was analyzed in a 7500 Real Time PCR System (Applied Biosystems) using SYBR premix EX TAQ II kit (Takara). $2^{-\Delta\Delta Ct}$ method was used to analyze the relative expression level and GAPDH was used as the internal reference gene. All primer sequences were synthesized and purchased from Shanghai Sangon Biotechnology Co., Ltd. (Shanghai, China):

SHPK1, F-TGCTGATGGCCTGATTGTCTT;
R-CTACAGGGAGGTAGGCCAGT.
IL1B, F-ATGATGGCTTATTACAGTGGCAA;
R-GTCGGAGATTCGTAGCTGGA.
TNFα, F-CAGGCGGTGCCTATGTCTC;
R-CGATCACCCCGAAGTTCAGTAG.
IFN-ɤ, F-GCCACGGCACAGTCATTGA,
R-TGCTGATGGCCTGATTGTCTT.

ELISA experiments

MDA, SOD, GSH, GSH-PX, ROS, IL-1β, IL-6,

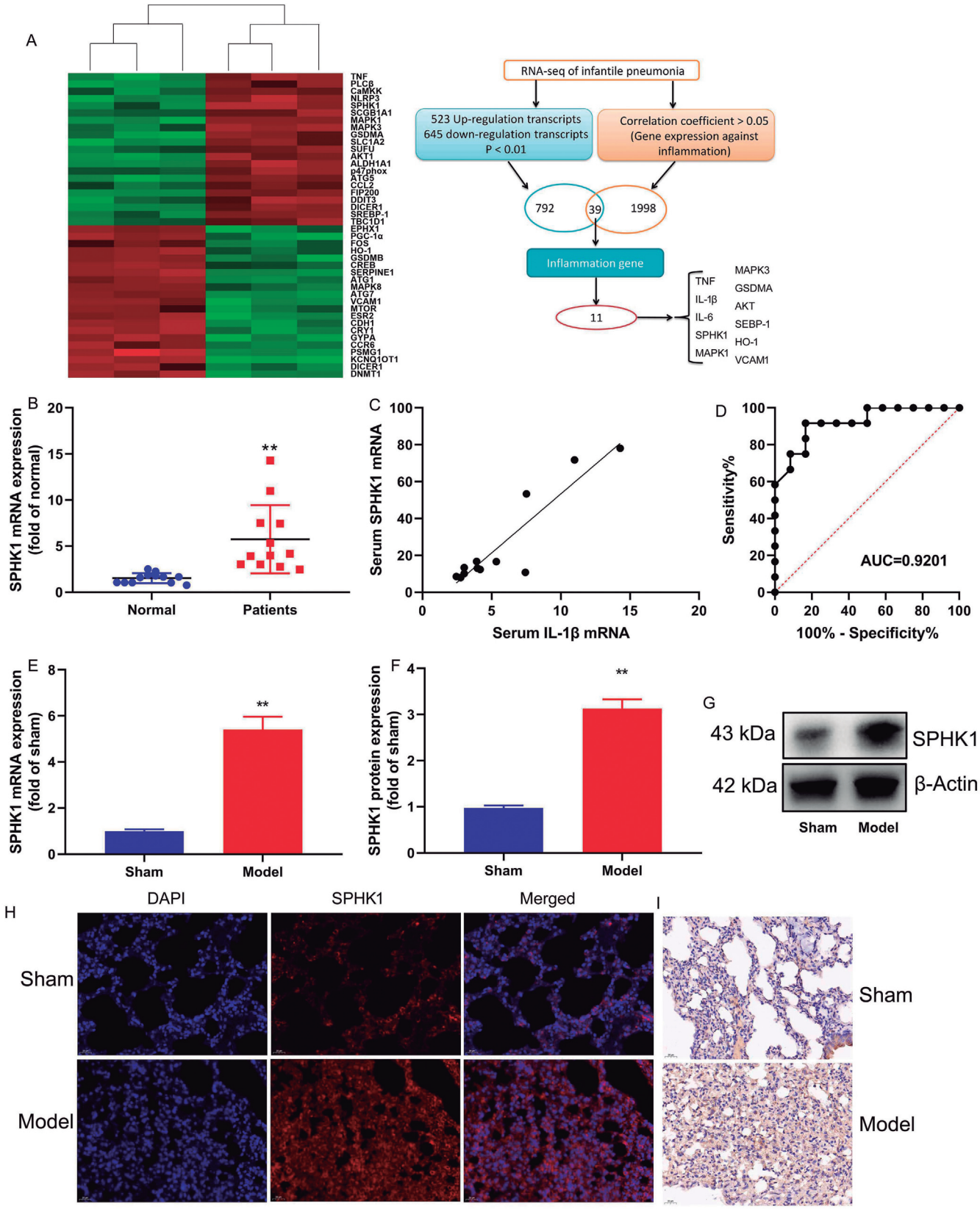

Fig 1. SPHK1 is upregulated in infantile pneumonia. Heat map showing the differential expressed genes related to inflammation between healthy controls (Left) and infantile pneumonia (Right) **(A)**, serum mRNA of SPHK1 between healthy control and patients **(B)**, serum mRNA of SPHK1 was correlation with serum IL-1β levels **(C)**, Sensitivity analysis by AUC - ROC curve in patients with infection **(D)**, lung tissue of SPHK1 mRNA expression in mouse model **(E)**, SPHK1 protein expression in lung tissues of mouse model **(F-G)**, SPHK1 protein expression (Immunohistochemistry, H), SPHK1 protein expression (Immunofluorescence, I) in the lung tissues of mouse model. Normal, healthy group; Patients, Patients with infantile pneumonia; Sham, sham control group; model, mice with infantile pneumonia. **p<0.01 compared with heathy control group or sham control group.

TNF-α and INF-γ levels in cultured supernatants were quantified using an ELISA kits according to the manufacturer's instructions. All the kits were purchased from Abcam (United Kingdom). OD values at 450 nm were determined by a microplate reader (Thermo Fisher Scientific).

Western blot

Lung tissue or cells were lysed in RIPA lysis buffer containing protease inhibitor (Thermo Fisher Scientific) on ice for 15 min. Protein concentrations in the lysate were determined by a BCA Protein assay kit (Beyotime Biotechnology, China). 10 ug of protein samples were separated by 10% SDS-PAGE and blotted on PVDF membrane. Membranes were blocked with 10% non-fat milk in TBST buffer at room temperature for 2h, and incubated with primary antibodies: SPHK1 (ab109522, 1:1000, abcam), SIRT1 (ab189494, 1:1000, abcam), NLRP3 (ab263899, 1:1000, abcam) and β-Actin (sc-8432, 1:5000, abcam) at 4°C overnight. After 4 times wash with TBST buffer, the membranes were further incubated with horseradish peroxidase–labeled secondary IgG (dilution 1:1000, abcam). The protein bands were developed using ECL western blotting detection reagent (GE Healthcare, USA), and photographed on a gel imager system (Bio-Rad, United States). The densitometry analysis was performed with Image J software (Bethesda, USA).

Statistical analysis

All data in the study were evaluated with SPSS version 18.0 software. Difference was considered as significant with a P value <0.05. The statistical difference between two groups was compared using unpaired student's t tests. Comparisons among multiple groups were analyzed using one-way analysis of variance (ANOVA) with Tukey's post hoc test for pairwise comparison.

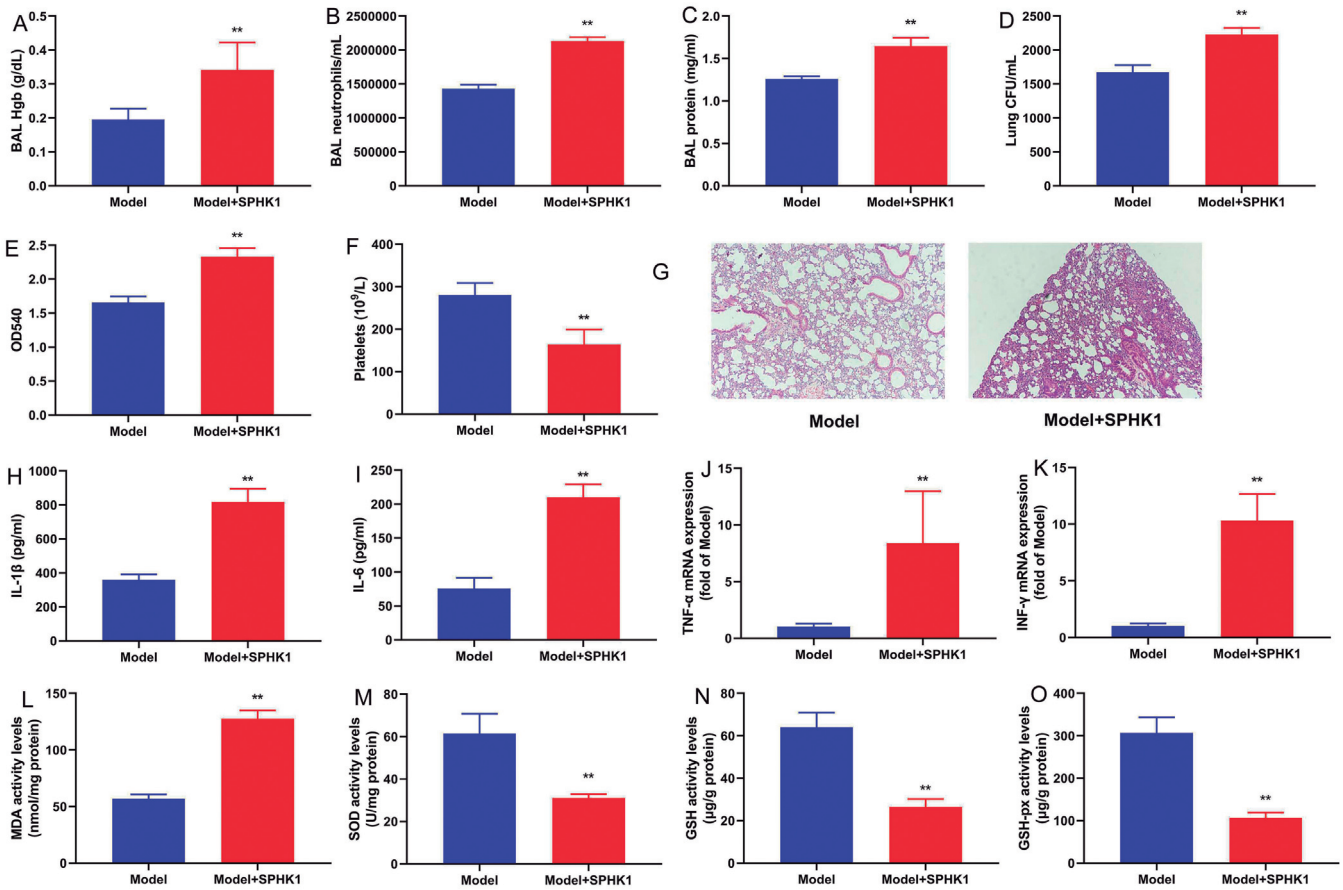

Fig. 2. SPHK1 protein promotes inflammation and lung injury in mice with infantile pneumonia. Bronchoalveolar lavage (BAL) Hemoglobin (Hgb) level **(A)**, BAL neutrophils **(B)**, BAL protein concentrations **(C)**, lung bacterial CFU **(D)**, BAL fluid turbidity OD540 **(E)**, circulating platelet counts **(F)**, lung tissue H&E staining **(G)**, IL-1β (K), IL-6 **(L)**, INF-γ **(M)**, TNF-α **(N)**, MDA **(L)**, SOD **(M)**, GSH **(N)**, GSH-PX **(O)** levels between infantile pneumonia group and the group treated with recombinant SPHK1 protein. Model: infantile pneumonia model mice group; Model+SPHK1: infantile pneumonia model mice with human SPHK1 recombinant protein; **p<0.01 compared between Model and Model+SPHK1 group.

Results

SPHK1 is upregulated the clinical samples and mouse model of infantile pneumonia

To identify the genes differentially expressed between healthy controls and patients, we used gene chip to analyze the expression of genes related to inflammatory responses. The analysis showed that SHPK1 is among the top inflammatory genes upregulated in pneumonia group (Fig. 1A). Then qRT-PCR result validated that serum level of SPHK1 mRNA was increased in patients with infantile pneumonia (Fig. 1B). Serum mRNA of SPHK1 was positively correlated with serum IL-1β level in patients with infantile pneumonia, with an ROC (Receiver operating characteristic) =0.9201 (Fig. 1C,D). We also confirmed the upregulation of SPHK1 mRNA and protein in the lung tissues of the mouse model of infantile pneumonia (Fig. 1E-G). Furthermore, immunohistochemistry and immunofluorescence analysis showed that SPHK1 expression in lung tissue was increased in mice with infantile pneumonia (Fig. 1H,I). Together, these data suggest that in the lung tissues of infantile pneumonia, SPHK1 upregulated is correlated with inflammation.

SPHK1 overexpression promotes inflammation and exacerbated lung injury in mice with infantile pneumonia

To determine the function of SPHK1 in infantile pneumonia, human SPHK1 recombinant protein was injected together with LPS into lung tissues of mice. Human SPHK1 protein increased hemoglobin (Hgb) protein concentrations and neutrophil infiltration in Bronchoalveolar lavage (BAL) fluid (Fig. 2A,B). The total protein level, bacterial load and turbidity (OD540) in BAL fluid were also increased by SPHK1 treatment (Fig. 2C,D), while the platelet level was reduced (Fig. 2F). H&E staining showed that SPHK1 increased lung tissue damages (Fig. 2G). Meanwhile, human SPHK1 protein increased the levels of inflammatory cytokines in BAL fluid, including TNF-α, INF-γ, IL-1β, and IL-6

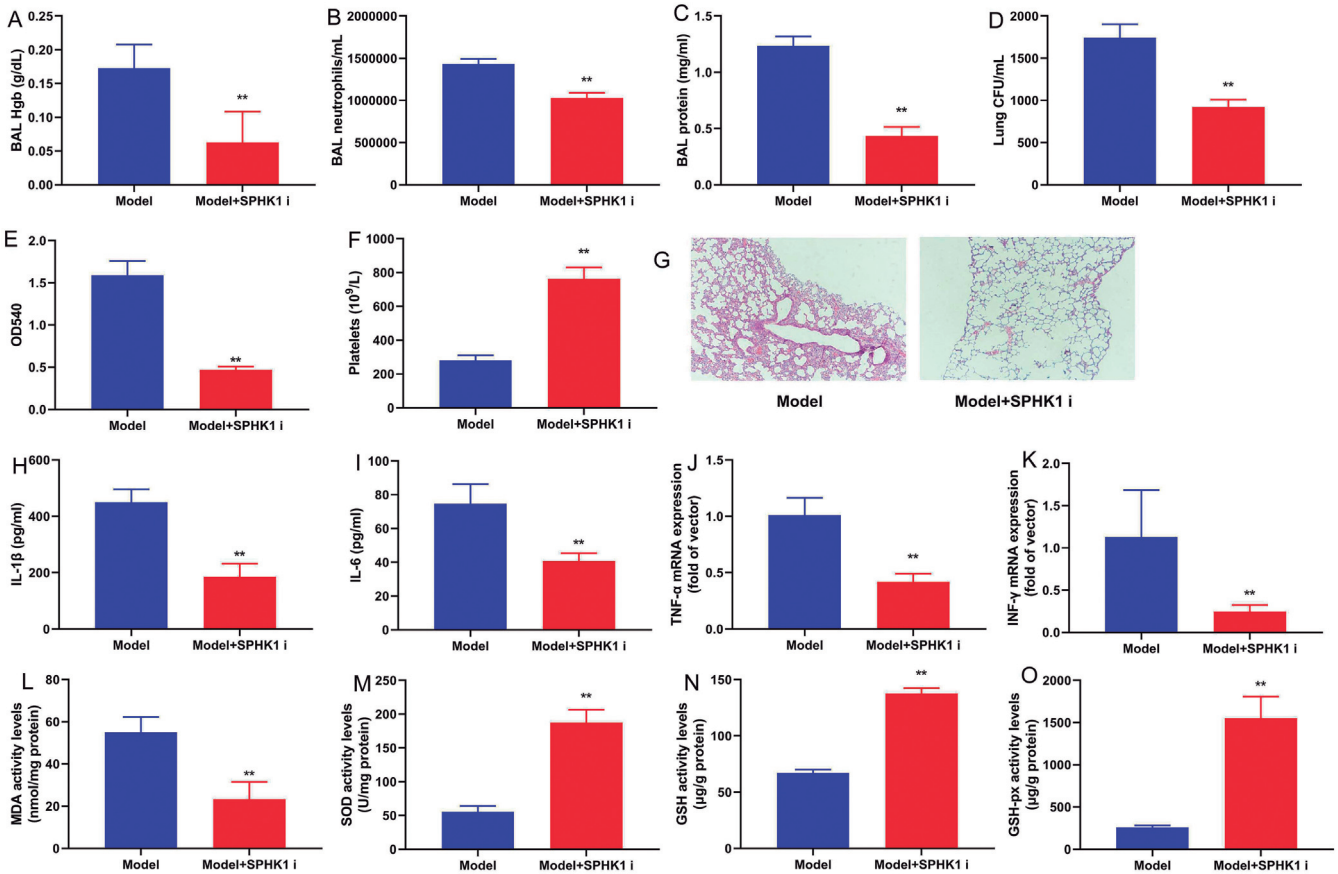

Fig. 3. The inhibition of SPHK1 activity suppresses inflammation and lung injury in mice with infantile pneumonia. Bronchoalveolar lavage (BAL) Hemoglobin (Hgb) level **(A)**, BAL neutrophils **(B)**, BAL protein concentrations **(C)**, lung bacterial CFU **(D)**, BAL fluid turbidity OD540 **(E)**, circulating platelet counts **(F)**, lung tissue H&E staining **(G)**, IL-1β **(K)**, IL-6 **(L)**, INF-γ **(M)**, TNF-α **(N)**, MDA **(L)**, SOD **(M)**, GSH **(N)**, GSH-PX **(O)** levels between infantile pneumonia group and the group treated with SPHK1 inhibitor. protein. Model, infantile pneumonia model mice group; Model+SPHK1 i, infantile pneumonia model mice with SPHK1 inhibitor group; **p<0.01 compared between Model and Model+SPHK1 I group.

(Fig. 2H-K). SPHK1 also induced oxidative stresses, as revealed by the increased MDA (Malondialdehyde) level, and reduced levels of GSH-PX (Plasma glutathione peroxidase), SOD (Superoxide dismutase) and GSH (glutathione) in the BAL fluid. (Fig. 2L-O).

Silencing SPHK1 inhibits inflammation and lung injury in mice with infantile pneumonia

We next applied SPHK1 inhibitor (MP-A08) to investigate whether inhibition of SPHK1 activity could protect the lung injury in mice with infantile pneumonia. SPHK1 inhibitor decreased hemoglobin (Hgb) protein concentrations and neutrophil infiltration in Bronchoalveolar lavage (BAL) fluid (Fig. 3A,B). The total protein level, bacterial load and turbidity (OD540) in BAL fluid were also decreased by SPHK1 inhibition (Fig. 3C,D), while the platelet level was increased (Fig. 3F). H&E staining showed that SPHK1 inhibition alleviated lung tissue damages (Fig. 2G). Meanwhile, SPHK1 inhibitor suppressed the levels of inflammatory cytokines in BAL fluid, including TNF-α, INF-γ, IL-1β, and IL-6 (Fig. 3H-K). SPHK1 inhibition also reduced oxidative stresses, as evidenced by the decreased MDA level, and elevated levels of GSH-PX, SOD and GSH in the BAL fluid. (Fig. 2L-O). These results suggests that SPHK1 promotes inflammation and lung injury of infantile pneumonia.

SPHK1 overexpression promotes inflammatory responses in RAW264.7 macrophage cells

Macrophages are key mediators of lung inflammation. To explore the roles of SPHK1 in macrophage, we transfected RAW264.7 cells with SPHK1 plasmid or SPHK1 siRNA and then stimulated the cells with LPS. As expected, SPHK1 level was increased by SPHK1 plasmid transfection, and si-SPHK1 reduced SPHK1 expression (Fig. 4A,B). Over-expression of SPHK1 increased IL-1β and IL-6 level in cell culture medium, as well as the mRNA levels of TNF-α and INF-γ in RAW264.7 cells stimulated with LPS (Fig. 4C-F). In contrast, silencing SPHK1 reduced IL-1β and IL-6 levels, and the mRNA expression of TNF-α and INF-γ model (Fig. 4G-J). Together, these data suggest SPHK1 promotes inflammatory responses in RAW264.7 macrophage cells.

SPHK1 promotes NLRP3 level but suppresses SIRT1 expression

To investigate the mechanism of SPHK1 mediated-inflammation, we analyzed the expression of genes after silencing SPHK1 treatment in RAW264.7 cells. We found that SIRT1 was upregulated and NLRP3 was downregulated after SPHK1 silencing. Online bioinformatics tools (TargetScan, RegRNA) found that

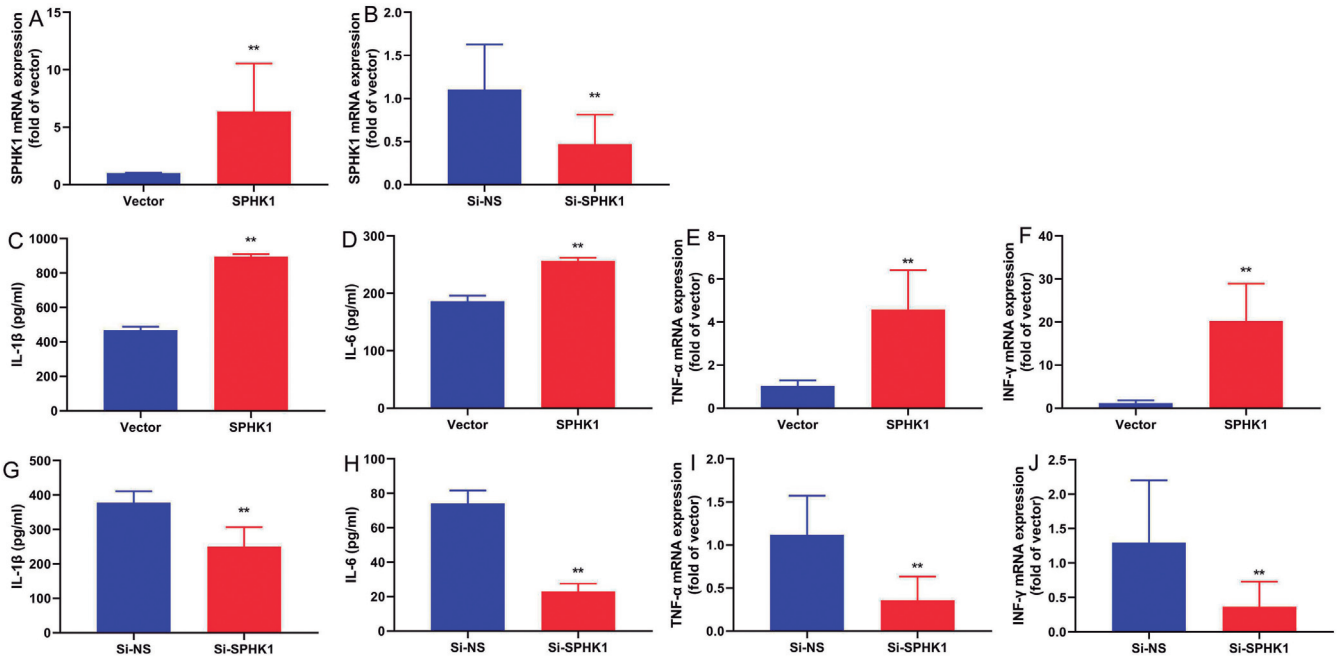

Fig. 4. SPHK1 regulates inflammation in an in vitro macrophage model. The expression level of SPHK1 **(A)**, IL-1β **(C)**, IL-6 **(D)**, INF-γ **(E)** and TNF-α **(F)** in RAW264.7 cells model after SPHK1 overexpression; The expression mRNA of SPHK1 **(B)**, IL-1β **(G)**, IL-6 **(H)**, INF-γ **(I)** and TNF-α **(J)** in RAW264.7 cells model after SPHK1 silencing; Vector, negative control group; SPHK1, over-expression of SPHK1; Si-NS, control siRNA group; Si-SPHK1, SPHK1 siRNA group. **p<0.01 compared with control group and experimental group.

SIRT1 and NLRP3 might interact with SPHK1 (Fig. 5A-C). Recombinant SPHK1 protein suppressed SIRT1 level and increased NLRP3 level in lung tissue of infantile pneumonia (Fig. 5D-F). And SPHK1 inhibitor treatment increased SIRT1 level but suppressed NLRP3 level in lung tissue of infantile pneumonia (Fig. 5G-I). These data suggest that SPHK1 promotes NLRP3 level but suppresses SIRT1 expression.

SPHK1 promotes inflammation by activating NLRP3 inflammasome and regulating mitochondrial permeability transition

The overexpression of SPHK1 increased SPHK1 and NLRP3 protein expressions and suppressed the protein expression of SIRT1 in macrophage cells (Fig. 6A). The overexpression of SPHK1 increased mitochondrial damage and stimulate the protein expression of NLRP3 in macrophage model (Fig. 6B). Overexpression of SPHK1 increased the production of ROS and MDA, and reduced SOD level and JC-1 staining (Fig. 6C-G).

In contrast, silencing SPHK1 decreased the expression of SPHK1 and NLRP3, but promoted the expression of SIRT1 (Fig. 6H). Silencing SPHK1 reduced mitochondrial damage and suppressed NLRP3 expression in macrophage stimulated by LPS (Fig. 6I). SPHK1 knockdown also decreased ROS production and

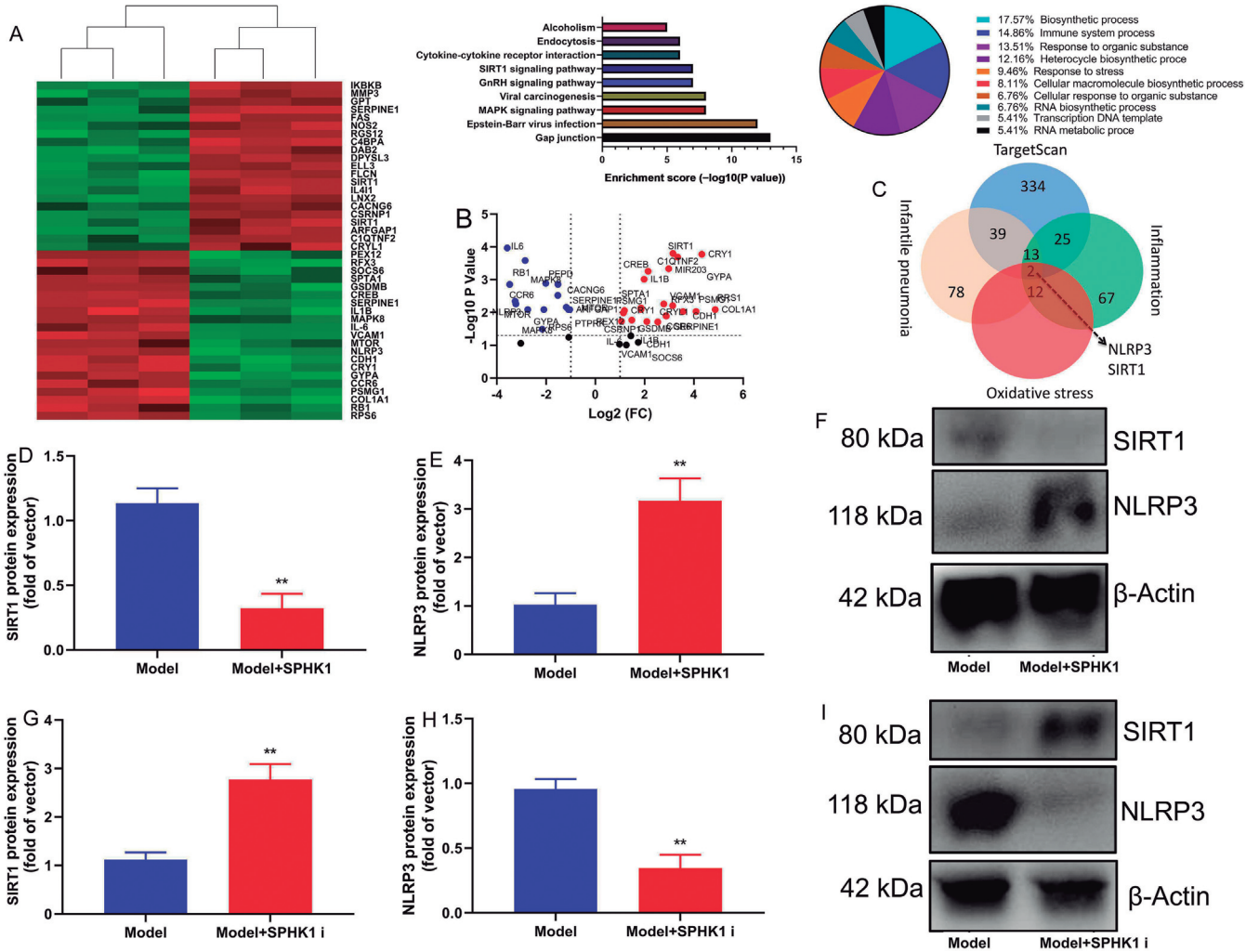

Fig. 5. SPHK1 suppress SIRT1 expression to reduce NLRP3 inflammasome activity by the inhibition of ROS-induced mitochondrial permeability transition. To investigate the mechanism of SPHK1 mediated-inflammation, we analyzed the expression of genes after silencing SPHK1 treatment in RAW264.7 cells. SIRT1 was upregulated and NLRP3 was downregulated after SPHK1 silencing in Heat map **(A)**, volcanic plot **(B)**, Online bioinformatics tools (TargetScan, RegRNA) found that SIRT1 and NLRP3 might interact with SPHK1 **(C)**, SIRT1 and NLRP3 protein expression in mice of infantile pneumonia with human SPHK1 recombinant protein treatment **(D-F)**; SIRT1 and NLRP3 protein expression in mice of infantile pneumonia with SPHK1 inhibitor treatment **(G-I)**. Model, infantile pneumonia model mice group; Model+SPHK1, infantile pneumonia model mice with human SPHK1 recombinant protein group; Model+SPHK1 i, infantile pneumonia model mice with SPHK1 inhibitor treatemnt; **p<0.01 compared between model and SPHK1 or SPHK1 I group.

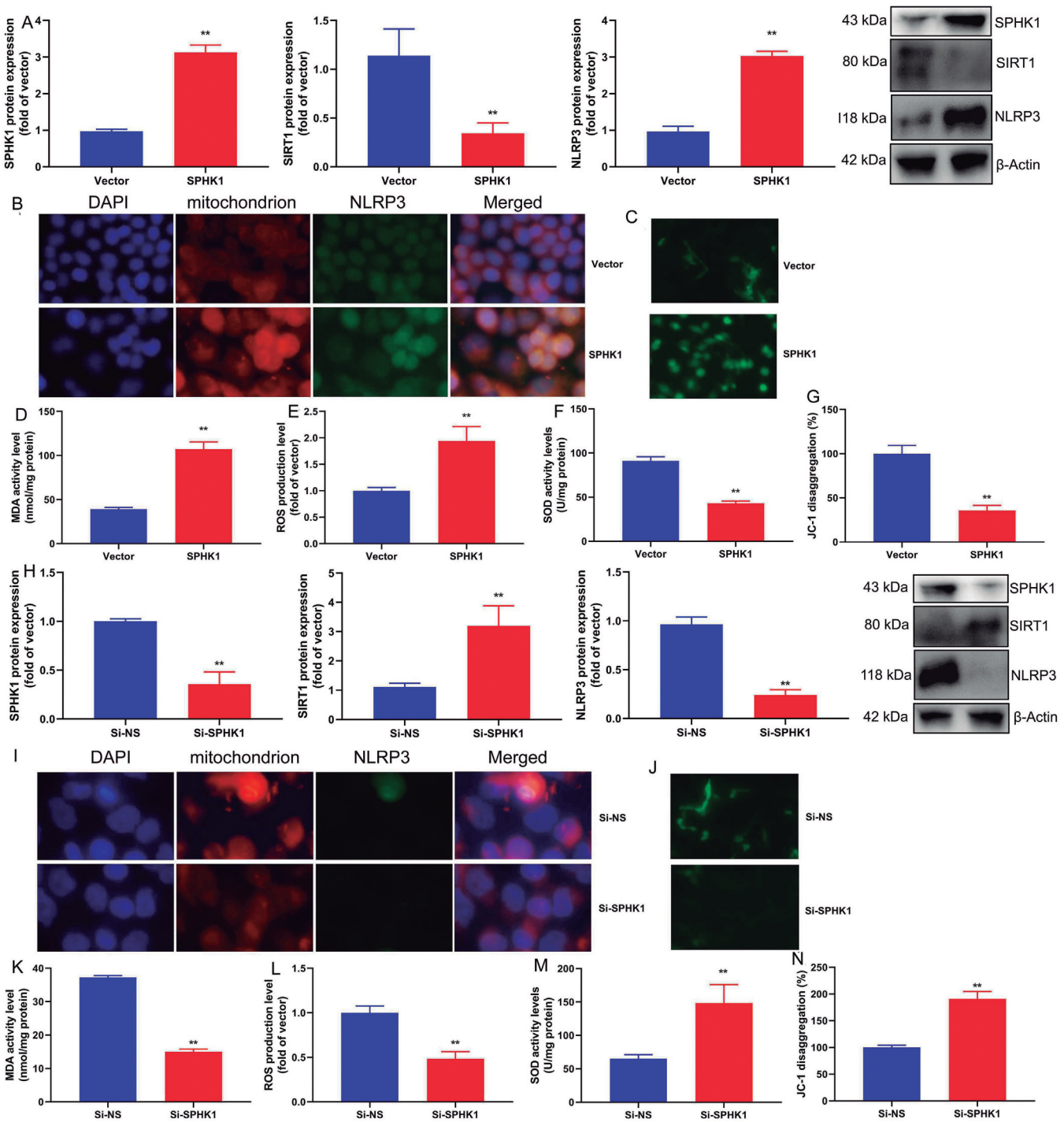

Fig. 6. SPHK1 promotes inflammation of infantile pneumonia by upregulating NLRP3 inflammasome and downregulating SIRT1. SPHK1, SIRT1 and NLRP3 protein expression upon SPHK1 overexpression in RAW264.7 macrophage cells **(A)**, mitochondrial permeability transition and NLRP3 expression in macrophage cells after SPHK1 overexpression **(B)**, ROS production **(C, E)**, MDA **(D)**, SOD **(F)** and JC-1 disaggregation levels **(G)** after SPHK1 overexpression. SPHK1, SIRT1 and NLRP3 protein expression **(H)**, mitochondrial permeability transition and NLRP3 expression **(I)**, ROS production **(J, L)**, MDA **(K)**, SOD **(M)** and JC-1 disaggregation levels **(N)** in RAW264.7 macrophage cells after silencing SPHK1. Vector, negative control group; SPHK1, over-expression of SPHK1; Si-NS, negative control siRNA group; Si-SPHK1, SPHK1 siRNA group. **p<0.01 compared with control group and experimental group.

MDA level, and increased SOD level and JC-1 staining in macrophages model (Fig. 6J-N). These results suggest that SPHK1 promotes inflammatory responses in macrophage by inducing NLRP3 inflammasome and impairing mitochondrial function via downregulating SIRT1.

SPHK1 regulates SIRT1 function in mouse model of infantile pneumonia

To confirm the role of SIRT1 in mouse model of infantile pneumonia, SIRT1 agonist (CAY10602) was applied together with SPHK1 protein after LPS injection. SIRT1 agonist lowered the protein level of NLRP3, reduced lung injury and IL-1β level (Fig. 7A-D). SIRT1 agonist treatment also decreased the MDA level, and increased GSH-PX, SOD and GSH activity levels in model of infantile pneumonia with human SPHK1 protein treatment (Fig. 7E-H). In contrast, SIRT1 inhibitor (Selisistat) caused opposite effects, including the increase of NLRP3 protein expression, enhanced lung injury and IL-1β level as well as augmented oxidative stresses (Fig. 7I-P).

Similarly, in the macrophage cell model, we found that SIRT1 agonist (20 μM) suppress NLRP3 protein expression, induced SIRT1 protein expression and

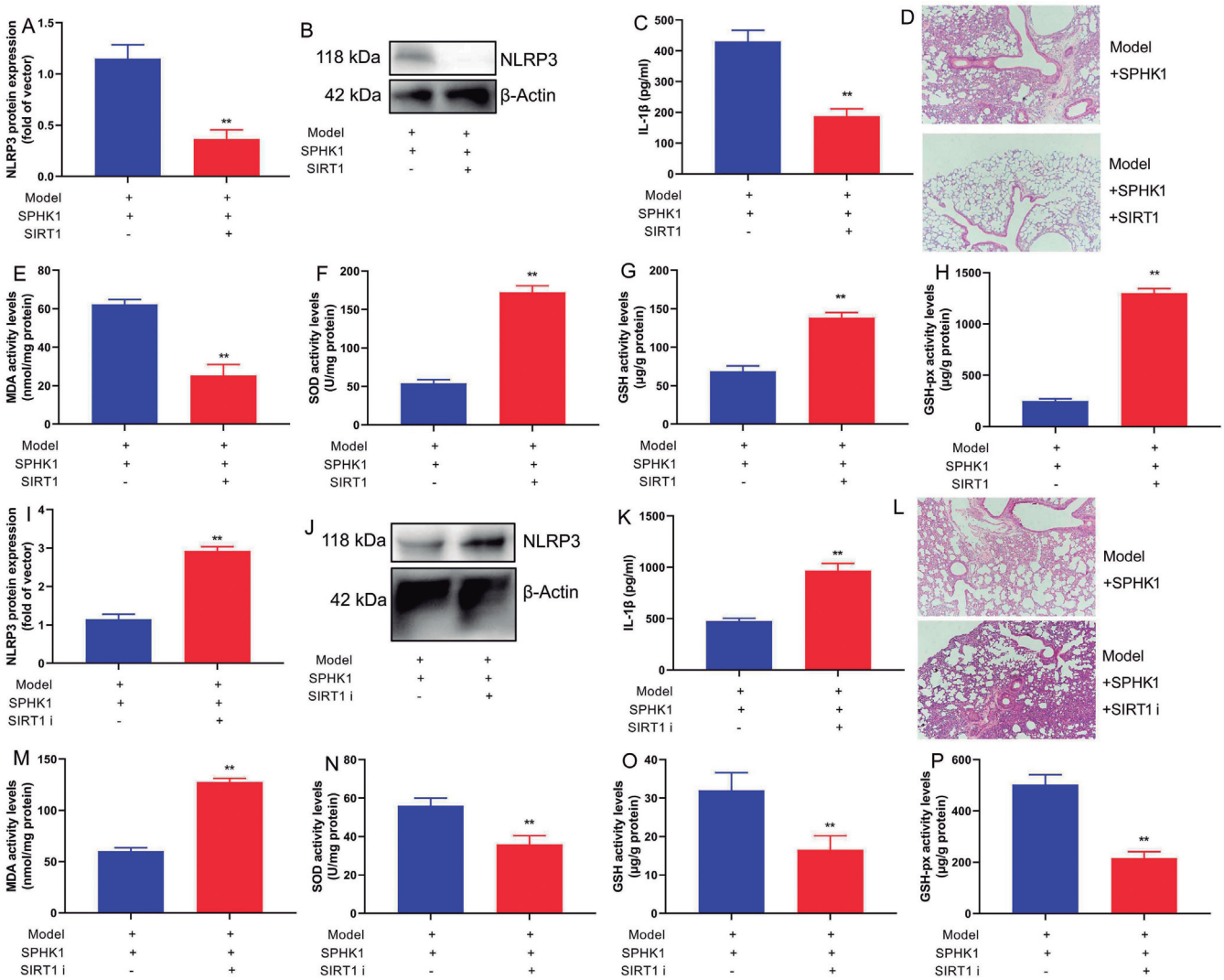

Fig. 7. SPHK1 regulates SIRT1 expression in mice model of infantile pneumonia. NLRP3 protein expression **(A, B)**, IL-1β level **(C)**, lung injury **(D)**, MDA level **(E)**, SOD level **(F)**, GSH level **(G)** and GSH-PX **(H)** activity levels in mice of infantile pneumonia with SPHK1 recombinant protein and SIRT1 Agonist treatment; NLRP3 protein expression **(I, J)**, IL-1β **(K)**, lung injury **(L)**, MDA **(M)**, SOD **(N)**, GSH **(O)** and GSH-PX **(P)** activity levels in mice of infantile pneumonia with SPHK1 recombinant protein and SIRT1 inhibitor treatment; Model+ SPHK1, infantile pneumonia model mice with human SPHK1 recombinant protein group; Model+SPHK1+SIRT1, infantile pneumonia model mice with SPHK1 recombinant protein and SIRT1 Agonist; Model+SPHK1+SIRT1 i, infantile pneumonia model mice with SPHK1 recombinant protein and SIRT1 inhibitor. **p<0.01 compared with model and SPHK1+SIRT1 or SPHK1+SIRT1 group.

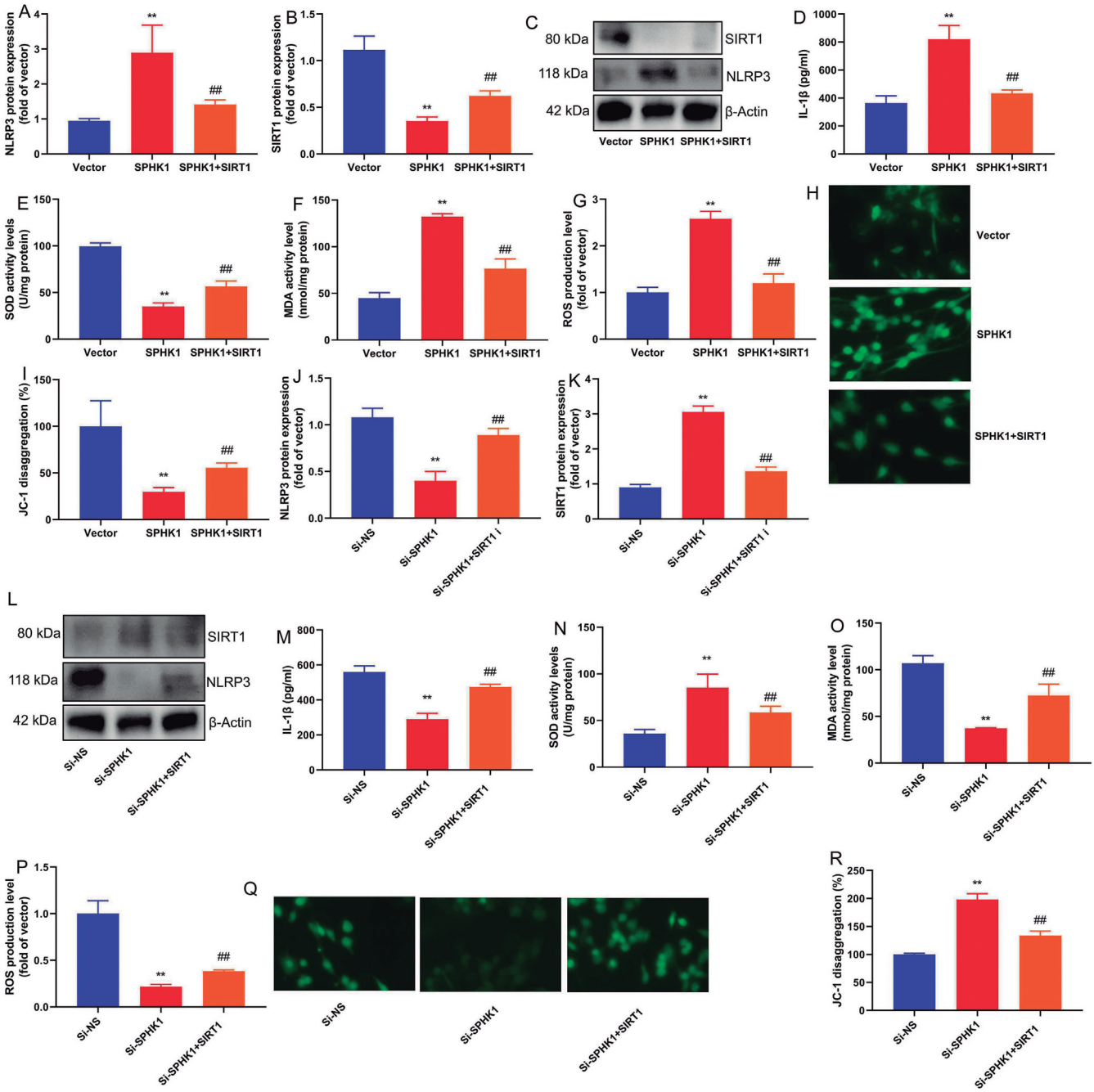

Fig. 8. SPHK1 regulates SIRT1 expression in RAW264.7 macrophage cells. SIRT1 and NLRP3 protein expression **(A-C)**, IL-1β **(D)**, SOD **(E)**, MDA **(F)**, ROS **(G, H)** and JC-1 disaggregation levels **(I)** in RAW264.7 macrophage cell model after SPHK1 overexpression and SIRT1 Agonist treatment; SIRT1 and NLRP3 protein expression **(J-L)**, IL-1β **(M)**, SOD **(N)**, MDA **(O)**, ROS **(P, Q)** and JC-1 disaggregation levels **(R)** in RAW264.7 macrophage cell model after SPHK1 silencing and SIRT1 inhibitor treatment. Vector, negative control group; SPHK1, over-expression of SPHK1; SPHK1+SIRT1, over-expression of SPHK1 and SIRT1 Agonist; Si-NS, Si-negative control group; Si- SPHK1, SPHK1 silencing group; Si-SPHK1+SIRT1 i, SPHK1 silencing and SIRT1 inhibitor group; **p<0.01 compared with control group or Si-negative control group; ##p<0.01 compared with over-expression of SPHK1 or SPHK1 silencing group.

reduced IL-1β level and oxidative stresses (Fig. 8A-G). SIRT1 agonist also rescued JC-1 staining in macrophages model with SPHK1 overexpression (Fig. 8I). While SIRT1 inhibitor (10μM) generate opposite effects on macrophages model with SPHK1 knockdown, by exacerbating inflammatory responses and oxidative stresses (Fig. 8J-R).

SPHK1 controls ROS-induced mitochondrial permeability transition in model of infantile pneumonia

To assess the role of ROS in model of infantile pneumonia, ROS inhibitor (5-Galloylquinic acid) was applied after SPHK1 treatment. ROS inhibitor suppressed the NLRP3 protein expression and IL-1β level, alleviated lung injury in mice of infantile pneumonia with SPHK1 recombinant protein treatment (Fig. 9A-D). ROS inhibitor also reduced GSH-PX, SOD and GSH levels, and augmented the activity of MDA level in mice of infantile pneumonia with SPHK1 protein treatment (Fig. 9E-H). In contrast, ROS agonist (Sideroxylin) increased NLRP3 protein expression and IL-1β level, exacerbated lung injury, and induced oxidative stresses in in mice of infantile pneumonia (Fig. 9I-P).

Notably, ROS inhibitor also suppressed NLRP3

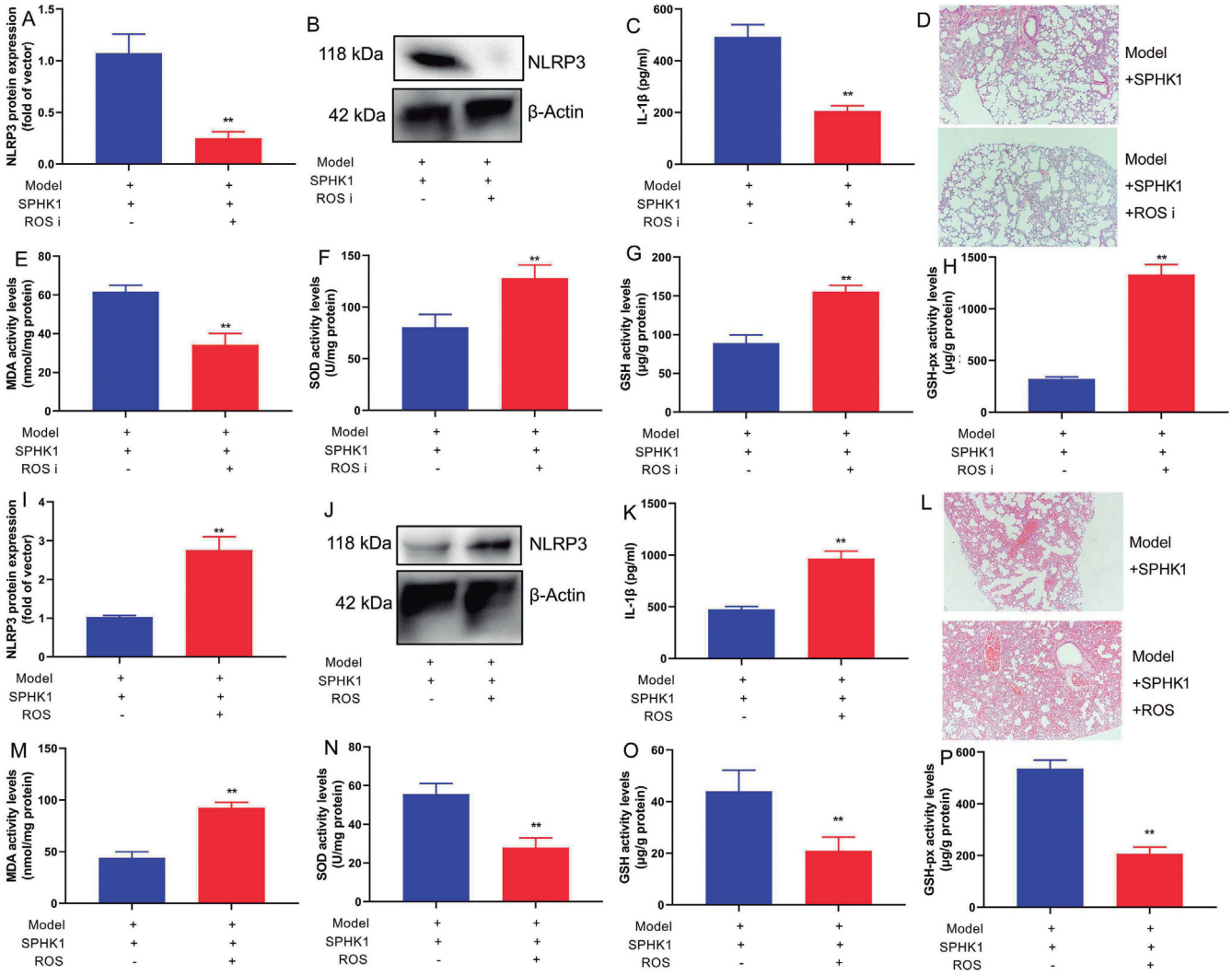

Fig. 9. SPHK1 controls ROS-induced mitochondrial permeability transition in mice model of infantile pneumonia. NLRP3 protein expression **(A, B)**, IL-1β **(C)**, lung injury **(D)**, MDA **(E)**, SOD **(F)**, GSH **(G)** and GSH-PX **(H)** activity levels in mice of infantile pneumonia with SPHK1 recombinant protein and ROS inhibitor; NLRP3 protein expression **(I, J)**, IL-1β (K), lung injury **(L)**, MDA **(M)**, SOD **(N)**, GSH **(O)** and GSH-PX **(P)** activity levels in mice of infantile pneumonia with SPHK1 recombinant protein and ROS agonist. Model+SPHK1, infantile pneumonia model mice with human SPHK1 recombinant protein group; Model+SPHK1+ROS i, infantile pneumonia model mice with SPHK1 recombinant protein and ROS inhibitor; Model+SPHK1+ROS, infantile pneumonia model mice with SPHK1 recombinant protein and ROS Agonist. **p<0.01 compared with infantile pneumonia model mice group.

protein expression and IL-1β level, alleviated oxidative stresses and increased JLC-1 staining levels in macrophages with SPHK1 overexpression (Fig. 10A-H). ROS agonist generate opposite effects on macrophages model with SPHK1 knockdown, by exacerbating inflammatory responses and oxidative stresses (Fig. 10I-P).

Discussion

*Mycoplasma pneumonia*e is a type of prokaryotic microorganism without cell wall structure and is one of the most common pathogens for pediatric respiratory infections (Chen et al., 2012). Infantile pneumonia in children around school age is generally caused by MP infection (Grinspan et al., 2020). With the in-depth study of pathogenesis, children with infantile pneumonia not only show severe lung disease, but also present damages in multiple organs throughout the body (Guo et al., 2018). In this study, we demonstrated the upregulation of SPHK1 in patients with infantile pneumonia and the mice of infantile pneumonia. A previous study by Huang et al. suggests that SPHK1 regulates pulmonary fibrosis by modulating mitochondrial reactive oxygen species in lung fibroblasts (Huang et al., 2020). Our data suggest that SPHK1 upregulation in infantile pneumonia may contribute to the augmented inflammatory responses and oxidative stresses.

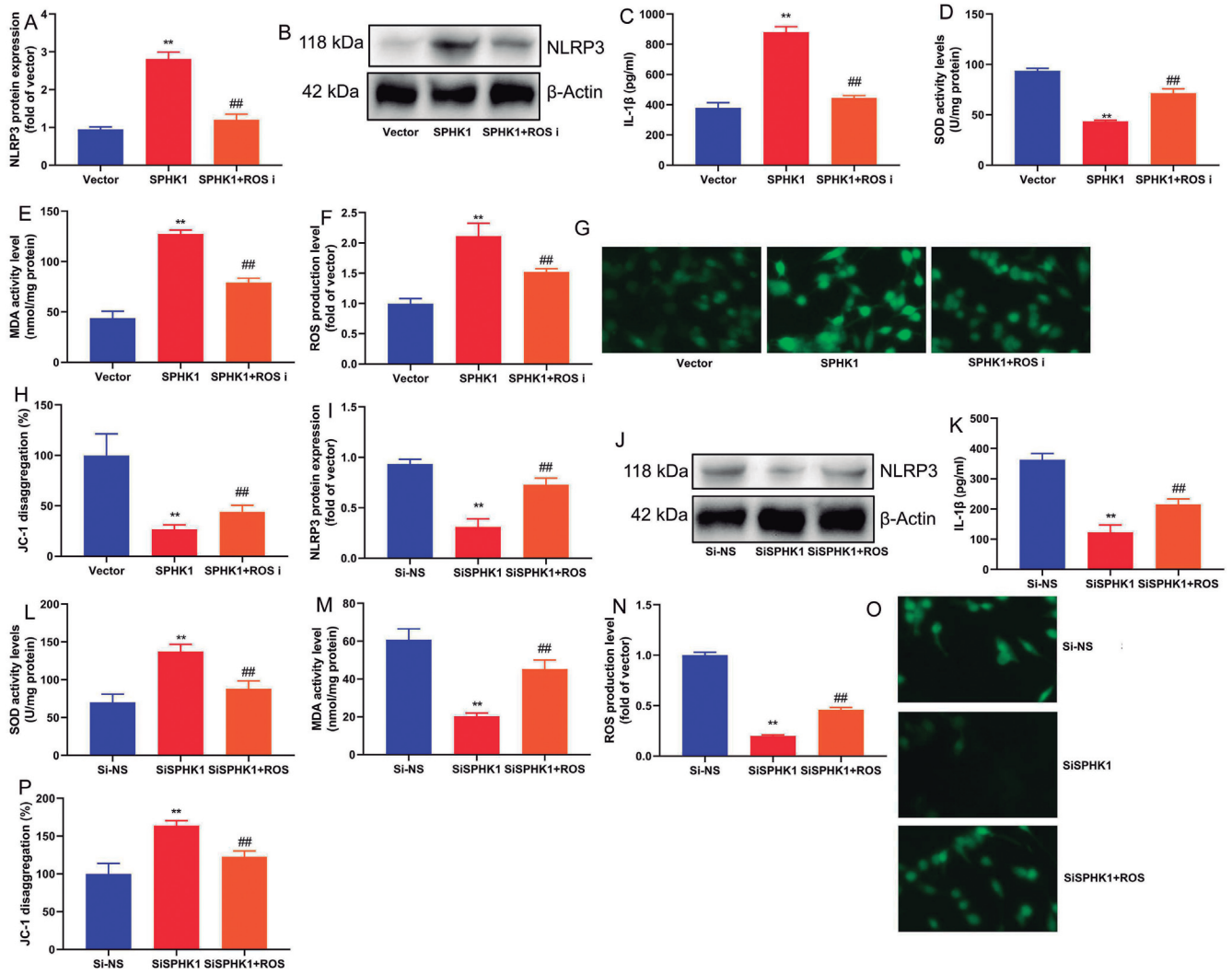

Fig. 10. SPHK1 controls ROS-induced mitochondrial permeability transition in RAW264.7 macrophage cells. NLRP3 protein expression **(A, B)**, IL-1β **(C)**, SOD **(D)**, MDA **(E)**, ROS **(F, G)** and JC-1 disaggregation levels **(H)** in RAW264.7 macrophage cells with SPHK overexpression and ROS inhibitor; NLRP3 protein expression **(I, J)**, IL-1β **(K)**, SOD **(L)**, MDA **(M)**, ROS **(N, O)** and JC-1 disaggregation levels **(P)** in RAW264.7 macrophage cells with SPHK silencing and ROS inhibitor; Vector, negative control group; SPHK1, over-expression of SPHK1; SPHK1+ROS i, over-expression of SPHK1 and ROS inhibitor; Si-NS, Si-negative control group; Si-SPHK1, SPHK1 silencing group; Si-SPHK1+ROS, SPHK1 silencing and ROS Agonist group; **p<0.01 compared with control group or Si-negative control group; ##p<0.01 compared with over-expression of SPHK1 or SPHK1 silencing group.

Oxidative stress is widely present in the body and plays an important physiological function (Delgado-Roche and Mesta, 2020). Under pathogen infection and other adverse stimuli, the excessive free radicals can cause oxidative damages by targeting different intracellular molecules and components (Iddir et al., 2020). Studies have shown that after adsorption on the cell membrane surface, *Mycoplasma pneumoniae* can modulate the release of hydrogen peroxide and superoxide radicals (Valavanidis et al., 2013; Zhang et al., 2018). The lung injury caused by oxidative stress is correlated with the occurrence and development of infantile pneumonia (Dai et al., 2018). As our data suggested, SPHK1 recombinant protein promotes inflammation and oxidative stress in model of infantile pneumonia, while the inhibition of its activity suppresses these adverse responses. Liu et al. showed that SPHK1 promotes ulcerative colitis by inducing inflammatory responses (Liu and Jiang, 2020). All the above data indicate a critical role of SPHK1 protein in the inflammation of infantile pneumonia.

Inflammation is one of the key factors contributing to vascular dysfunction, endothelial cell apoptosis and aging (Ichikawa et al., 2013). A previous study showed that the expression level of SIRT1 in endothelial cells decreases with an impaired angiogenesis during aging (Lin et al., 2014). Endothelial cell aging is an important marker of vascular aging, which is also the main cause of cardiovascular diseases such as hypertension and atherosclerosis (Gallob et al., 2021). In our study, we observed that SPHK1 suppresses SIRT1 expression in the model of infantile pneumonia. Gao et al. reported that SIRT1 mediates SPHK1-induced endothelial cells proliferation and migration (Gao et al., 2016). Our data suggest that SPHK1 regulate inflammation and oxidative responses by regulating SIRT1 expression in infantile pneumonia. However, the mechanism underlying SIRT1 expression warrants further investigation.

NLRP3 inflammasome recognizes the corresponding molecular patterns and activates the release of various inflammatory factors such as IL-18 and IL-1β during inflammatory responses (Bai et al., 2020). Studies have shown that the early immune response to stimuli in the lung is mainly mediated by inflammasome (Liu et al., 2021; Luo et al., 2021a). However, excessive inflammation can aggravate tissue damages and lead to respiratory disorder (Tang et al., 2019). The occurrence and development of respiratory diseases is associated with inflammation, including infectious pneumonia, silicosis, asthma, chronic obstructive pulmonary disease (COPD) and ALI (acute lung injury) (Segovia et al., 2018), since excessive proinflammatory cytokines are detrimental to tissue homeostasis (Segovia et al., 2018; Pu et al., 2019). Zhong et al. showed that the silencing of SPHK1 reduces microvascular leakage through attenuating NLRP3 inflammasome in sepsis (Zhong et al., 2020). Our results also demonstrated that SPHK1 suppresses NLRP3 inflammasome in model of infantile pneumonia.

However, our study did not investigate how SPHK1 regulates NLRP3 expression in model of infantile pneumonia. Future work will need to delineate how SPHK1 modulates NLRP3 and SIRT1 expression in the mouse model of infantile pneumonia. In addition, since sphingosine phosphate-1 (S1P) production by SPHK1 may play a role in tissue damages such as liver fibrogenesis (Hart et al., 2019), future work will need to focus on whether S1P production is involved in SPHK1-mediated infantile pneumonia. It is worth mentioning that the SIRT1/NLRP3 axis might not be only signaling axis underlying the function of SPHK1 in the context of infantile pneumonia.

In conclusion, this study shows that SPHK1 promotes inflammation and oxidative stress in model of infantile pneumonia. Our findings suggest that SPHK1 suppresses SIRT1 expression to promote mitochondrial permeability transition and increases NLRP3 level to modulate inflammation in the model of infantile pneumonia. Together, our data suggest SIRT1/NLRP3 axis mediate the downstream inflammatory and oxidative effects of SPHK1 in infantile pneumonia, which provides insights into the development of novel therapeutic scheme for infantile pneumonia.

Acknowledgements. None.

Ethic approval. All the samples following patient consent were approval by the Ethics Committee of Hunan Children's Hospital.

Conflict of interest. All authors declare that they have no conflict of interest.

Informed consent. Serum of all patients and normal healthy volunteers were collected after sign the informed consent form.

References

Bai F., Wu J., Liu B., Wang X., Shi X., Lv T., Wang Y. and Hao Y. (2020). *Mycoplasma ovipneumoniae*-derived lipid-associated membrane proteins induce cytokine secretion in mouse peritoneal macrophages through TLR2 signalling. Res. Vet. Sci. 132, 474-480.

Chen C.H., Wen H.J., Chen P.C., Lin S.J., Chiang T.L., Hsieh I.C. and Guo Y.L. (2012). Prenatal and postnatal risk factors for infantile pneumonia in a representative birth cohort. Epidemiol. Infect. 140, 1277-12785.

Dai J., Gu L., Su Y., Wang Q., Zhao Y., Chen X., Deng H., Li W., Wang G. and Li K. (2018). Inhibition of curcumin on influenza A virus infection and influenzal pneumonia via oxidative stress, TLR2/4, p38/JNK MAPK and NF-κB pathways. Int. Immunopharmacol. 54, 177-187.

Delgado-Roche L. and Mesta F. (2020). Oxidative stress as key player in severe acute respiratory syndrome coronavirus (SARS-CoV) infection. Arch. Med. Res. 51, 384-387.

Gallob F., Brcic L., Eidenhammer S., Rumpp F., Nerlich A. and Popper H. (2021). Senescence and autophagy in usual interstitial pneumonia of different etiology. Virchows Arch. 478, 497-506.

Gao Z., Wang H., Xiao F.J., Shi X.F., Zhang Y.K., Xu Q.Q., Zhang X.Y., Ha X.Q. and Wang L.S. (2016). SIRT1 mediates Sphk1/S1P-induced proliferation and migration of endothelial cells. Int. J. Biochem. Cell Biol. 74, 152-160.

Grinspan Z.M., Mytinger J.R., Baumer F.M., Ciliberto M.A., Cohen B.H., Dlugos D.J., Harini C., Hussain S.A., Joshi S.M., Keator C.G., Knupp K.G., McGoldrick P.E., Nickels K.C., Park J.T., Pasupuleti A., Patel A.D., Pomeroy S.L., Shahid A.M., Shellhaas R.A., Shrey D.W., Singh R.K., Wolf S.M., Yozawitz E.G., Yuskaitis C.J., Waugh J.L. and Pearl P.L. (2020). Crisis standard of care: Management of infantile spasms during COVID-19. Ann. Neurol. 88, 215-217.

Guo S., Bao L., Qu T., Mao X., Gao Y., Xu Y. and Cui X. (2018). Ameliorative effects of infantile feire kechuan oral solution on *Mycoplasma pneumoniae pneumonia* in infant mouse and rat models. Evid. Based Complement Alternat. Med. 2018, 8139040.

Hart P.C., Chiyoda T., Liu X., Weigert M., Curtis M., Chiang C.Y., Loth R., Lastra R., McGregor S.M., Locasale J.W., Lengyel E. and Romero I.L. (2019). SPHK1 is a novel target of metformin in ovarian cancer. Mol. Cancer Res. 17, 870-881.

Huang L.S., Sudhadevi T., Fu P., Punathil-Kannan P.K., Ebenezer D.L., Ramchandran R., Putherickal V., Cheresh P., Zhou G., Ha A.W., Harijith A., Kamp D.W. and Natarajan V. (2020). Sphingosine kinase 1/S1P signaling contributes to pulmonary fibrosis by activating Hippo/YAP pathway and mitochondrial reactive oxygen species in lung fibroblasts. Int. J. Mol. Sci. 21, 2064.

Ichikawa T., Hayashi R., Suzuki K., Imanishi S., Kambara K., Okazawa S., Inomata M., Yamada T., Yamazaki Y., Koshimizu Y., Miwa T., Matsui S., Usui I., Urakaze M., Matsuya Y., Sasahara M. and Tobe K. (2013). Sirtuin 1 activator SRT1720 suppresses inflammation in an ovalbumin-induced mouse model of asthma. Respirology 18, 332-339.

Iddir M., Brito A., Dingeo G., Fernandez Del Campo S.S., Samouda H., La Frano M.R. and Bohn T. (2020). Strengthening the immune system and reducing inflammation and oxidative stress through diet and nutrition: Considerations during the COVID-19 Crisis. Nutrients 12, 1562.

Khoei S.G., Sadeghi H., Samadi P., Najafi R. and Saidijam M. (2020). Relationship between Sphk1/S1P and microRNAs in human cancers. Biotechnol. Appl. Biochem. 68, 279-287.

Lee J.Y., Han S.H., Park M.H., Baek B., Song I.S., Choi M.K., Takuwa Y., Ryu H., Kim S.H., He X., Schuchman E.H., Bae J.S. and Jin H.K. (2018). Neuronal SphK1 acetylates COX2 and contributes to pathogenesis in a model of Alzheimer's Disease. Nat. Commun. 9, 1479.

Li S., Cui W., Song Q., Zhou Y. and Li J. (2019). miRNA-302e attenuates inflammation in infantile pneumonia though the RelA/BRD4/NF-κB signaling pathway. Int. J. Mol. Med. 44, 47-56.

Lin L., Wen S.H., Guo S.Z., Su X.Y., Wu H.J., Chong L., Zhang H.L., Zhang W.X. and Li C.C. (2014). Role of SIRT1 in Streptococcus pneumoniae-induced human β-defensin-2 and interleukin-8 expression in A549 cell. Mol. Cell Biochem. 394, 199-208.

Liu J. and Jiang B. (2020). Sphk1 promotes ulcerative colitis via activating JAK2/STAT3 signaling pathway. Hum Cell. 33, 57-66.

Liu F., Liu T., Sun M., Zhou J., Xue F., Chen S., Chen J. and Zhang L. (2021). Maxing shigan decoction mitigates *Mycoplasma pneumonia*-induced pyroptosis in A549 cells via the NLRP3 inflammasome. Infect. Drug Resist. 14, 859-867.

Luo H., He J., Qin L., Chen Y., Chen L., Li R., Zeng Y., Zhu C., You X. and Wu Y. (2021a). *Mycoplasma pneumoniae* lipids license TLR-4 for activation of NLRP3 inflammasome and autophagy to evoke a proinflammatory response. Clin. Exp. Immunol. 203, 66-79.

Luo X., Chang X., Zhou H., Lin H. and Fan H. (2021b). *Glaesserella parasuis* induces inflammatory response in 3D4/21 cells through activation of NLRP3 inflammasome signaling pathway via ROS. Vet. Microbiol. 256, 109057.

Pu Z., Han C., Zhang W., Xu M., Wu Z., Liu Y., Wu M., Sun H. and Xie H. (2019). Systematic understanding of the mechanism and effects of Arctigenin attenuates inflammation in dextran sulfate sodium-induced acute colitis through suppression of NLRP3 inflammasome by SIRT1. Am. J. Transl. Res. 11, 3992-4009.

Pu Z., Liu Y., Li C., Xu M., Xie H. and Zhao J. (2020). Using network pharmacology for systematic understanding of geniposide in ameliorating inflammatory responses in colitis through suppression of NLRP3 inflammasome in macrophage by AMPK/Sirt1 dependent signaling. Am. J. Chin. Med. 48, 1693-1713.

Pu Z., Shen C., Zhang W., Xie H. and Wang W. (2022). Avenanthramide C from oats protects pyroptosis through dependent ROS-induced mitochondrial damage by PI3K ubiquitination and phosphorylation in pediatric pneumonia. J. Agric Food Chem. 70, 2339-2353.

Segovia J.A., Chang T.H., Winter V.T., Coalson J.J., Cagle M.P., Pandranki L., Bose S., Baseman J.B. and Kannan T.R. (2018). NLRP3 is a critical regulator of inflammation and innate immune cell response during *Mycoplasma pneumoniae* Infection. Infect. Immun. 86, e00548-17.

Tang J., Li Y., Wang J., Wu Q. and Yan H. (2019). Polydatin suppresses the development of lung inflammation and fibrosis by inhibiting activation of the NACHT domain-, leucine-rich repeat-, and pyd-containing protein 3 inflammasome and the nuclear factor-κB pathway after Mycoplasma pneumoniae infection. J. Cell Biochem. 120, 10137-10144.

Tomari K., Morino S. and Horikoshi Y. (2018). Case of infantile legionella pneumonia after bathing in reheated and reused water. Pediatr. Infect Dis. J. 37, 370-372.

Valavanidis A., Vlachogianni T., Fiotakis K. and Loridas S. (2013). Pulmonary oxidative stress, inflammation and cancer: respirable particulate matter, fibrous dusts and ozone as major causes of lung carcinogenesis through reactive oxygen species mechanisms. Int. J. Environ Res. Public Health 10, 3886-3907.

Xiaomeng Z., Jiarui W., Bing Z. and Ling D. (2015). Potassium dehydroandrographolide succinate injection for treatment of infantile pneumonia: a systematic review and Meta-analysis. J. Tradit Chin. Med. 35, 125-133.

Zhang Q., Ju Y., Ma Y. and Wang T. (2018). N-acetylcysteine improves oxidative stress and inflammatory response in patients with community acquired pneumonia: A randomized controlled trial. Medicine (Baltimore) 97, e13087.

Zhang J., Wang C.H., Liu X.J., Cheng S.F., Han L.H. and Lv C.L. (2020). Efficacy and safety analysis of dopamine combined with creatine phosphate sodium in the treatment of infantile pneumonia combined with heart failure. J. Biol. Regul. Homeost. Agents 34, 2103-2108.

Zhong M., Wu W., Wang Y., Mao H., Song J., Chen S. and Zhu D. (2020). Inhibition of sphingosine kinase 1 attenuates sepsis-induced microvascular leakage via inhibiting macrophage NLRP3 inflammasome activation in mice. Anesthesiology 132, 1503-15.

Accepted July 7, 2022